

Green and scalable synthesis of porous carbon nanosheet-assembled hierarchical architectures for robust capacitive energy harvesting

Lu Guan¹, Lei Pan¹, Tingyue Peng, Tong Qian, Yunchun Huang, Xinxin Li, Cai Gao, Zhen Li, Han Hu^{*}, Mingbo Wu^{**}

State Key Laboratory of Heavy Oil Processing, Institute of New Energy, College of Chemical Engineering, China University of Petroleum (East China), Qingdao, 266580, China

ARTICLE INFO

Article history:

Received 12 March 2019
Received in revised form
30 May 2019
Accepted 13 June 2019
Available online 14 June 2019

ABSTRACT

Hierarchical carbon architectures offer superb advantages for energy storage, but their general synthesis requires tedious template methods and subsequent activation processes employing highly corrosive potassium hydroxide as the activation agent. Herein, we report a green and scalable production of the nanosheet-assembled hierarchical carbon architecture using potassium citrate as a green activation agent as well as an in-situ template and petroleum asphalt as the precursor. The replacing potassium hydroxide with potassium citrate can not only reduce the adverse impact on environment during the industrially scalable production but also eliminate the necessity of extra templates in traditional strategies. Meanwhile, the employment of petroleum asphalt as the carbon precursor can increase the yield of carbon, thus reducing the cost for constructing such structures. The as-prepared carbon architecture shows large specific surface area and hierarchical porosity. Besides, the porous carbon nanosheet facilitates efficient electrons/ions transfer which permits high-power handling. Because of these structure merits, the porous carbon nanosheet-assembled hierarchical architecture affords outstanding performance in terms of large specific capacitance, extraordinary rate capability, and long cyclic stability. The strategy demonstrated here may open up new possibilities for creating novel carbon nanostructures for energy-related application in cost-effective manners.

© 2019 Elsevier Ltd. All rights reserved.

1. Introduction

The rational design and construction of hierarchical carbon architectures have aroused widespread attention recently because of their pivotal roles in substantially boosting the performance of energy storage and conversion devices [1–10]. Specifically, the hierarchical porosity can simultaneously act as ion-buffer reservoirs, serve as rapid ion transfer channels, and provide abundant locations for ion accommodation, which contributes to robust capacitive energy harvesting for supercapacitors [11–14]. To essentially explore the potential of these structures for this purpose, tremendous efforts have been made in past decades with remarkable achievements [15–17]. Fan et al. reported the combination of soft template and KOH-mediated activation to construct nitrogen-

doped hierarchical porous carbon nanospheres as electrode materials for supercapacitors [18]. Using SiO₂ nanoparticles as templates, Hu and his colleague reported the designed formation of hierarchical carbon architecture through combining KOH activation [19].

The current progress indicates that most of these architectures are constructed through laborious procedures that include multi-step pore regulation. Generally, macropores are created through hard/soft template methods, while the meso-/micro-porosity is manipulated by chemical activation usually using potassium hydroxide as the activation agent. Despite the high controllability of these strategies, the processes are too costly for industrially scalable production. Moreover, the inevitable use of highly corrosive potassium hydroxide imposes great environmental impact on the production process. As a result, facile synthesis procedures employing environment-friendly agents are urgently required. M. Sevilla et al. reported that the direct pyrolysis of potassium citrate in inert atmosphere at elevated temperatures could contribute to carbon nanosheet-assembled hierarchical architecture [20].

* Corresponding author.

** Corresponding author.

E-mail addresses: hhu@upc.edu.cn (H. Hu), wumb@upc.edu.cn (M. Wu).

¹ These authors contributed equally to this work.

Because of the simplicity and straightforwardness, this method has been extensively exploited to increase the controllability for enhanced performance [21,22]. Considering the wide demand and scalable deployment of energy storage devices in the near future, the high-yield production of the key components for supercapacitors, namely carbon electrode materials, is desperately needed [23,24]. Nevertheless, the directly using potassium citrate as the precursor generally showcases a very low carbon yield which restricts the scalable use of this strategy. Therefore, alternative methods with not only simplicity but also high yield using cheap precursors remain to be exploited [25].

As a low-value byproduct during the petroleum processing, asphalt is produced at extremely large quantity [26]. The carbon content in asphalt is generally higher than that of many other precursors for carbon materials which may contribute to high-yield production. Besides, asphalt normally contains a large portion of polycyclic aromatic hydrocarbons rendering the as-prepared carbon with high conductivity, an extremely desirable property for advanced energy storage. Moreover, the melt and fluidity of asphalt at elevated temperatures provide an excellent opportunity of facilely introducing in-situ template for pore regulation [27–29].

Based on the aforementioned discussion, we propose a green and scalable production of nanosheet-assembled hierarchical carbon architecture (NHCA) through co-carbonizing potassium citrate and petroleum asphalt. At elevated temperatures, the potassium citrate decompose into potassium carbonate particles serving as templates which will guide the melted asphalt converting into interconnected carbon nanocages around them. The further increasing of the temperatures will result in the activation of carbon nanocages to produce large amount of micropores as well as mesopores. These structural merits render the as-prepared NHCAs with outstanding performance as electrodes for supercapacitors. Because of the low-cost, high-yield, and environment-friendly properties, the strategies suggested here may contribute to a new avenue for construction of novel carbon materials with potential for practical energy storage application.

2. Experimental

2.1. Preparation of NHCAs

Petroleum asphalt was obtained from Sinopec Group (7.1 wt % saturates, 24.9 wt % aromatics, 46.1 wt % resins and 18.0 wt % asphaltenes). Potassium citrate was bought from Aladdin Ltd. All other chemicals were of analytical grade and used without any further purification. In a typical synthesis, 1 g of petroleum asphalt was mixed with a certain amount of potassium citrate through grounding in an agate mortar for 10 min. Then, the mixture loaded in a corundum boat was transferred into a horizontal tube oven. A four-step heating procedure was applied, where the mixture was heated to 300 °C at a ramping rate of 5 °C min⁻¹ and held at 300 °C for 30 min, then to 800 °C with 5 °C min⁻¹ and remained at this temperature for another 120 min under N₂ atmosphere. After washing with water followed by drying at 60 °C for 10 h, the nanosheet-assembled hierarchical carbon architectures (NHCAs) were obtained. The as-prepared products were named as NHCA-X, where the X represent the mass ratio of potassium citrate to petroleum asphalt. Besides, potassium citrate has also been directly pyrolyzed as a reference sample denoted as HCA. Petroleum asphalt was also directly carbonized, denoted as petroleum asphalt-derived carbon (PAC), for comparison.

2.2. Characterization

The morphologies and microstructures of the as-prepared carbon materials were characterized by field-emission scanning electron microscopy (FESEM, Hitachi S-4800 Japan) and transmission electron microscopy (TEM, JEM-2100UHR, Japan). Energy dispersive X-ray spectroscopy (EDS) was carried out on an EDX system attached on the TEM system. The crystal structures and the synthesis mechanism of the NHCAs were explored by X-ray diffraction (XRD X'Pert PRO MPD, Holland). The surface functional groups and defects were studied by X-ray photoelectron spectroscopy (XPS, Thermo Scientific Escalab 250XI) and Raman spectroscopy (Renishaw RM2000), respectively. Pore structure and specific surface area were determined by nitrogen adsorption-desorption isotherms on a sorptometer (Micromeritics, ASAP 2020, USA). The specific surface area was obtained by BET (Brunauer-Emmett-Teller) equation and the total pore volume (V_t) was obtained under a relative pressure (P/P₀) of 0.99. The pore diameter was analyzed from the adsorption branches of the isotherms using the density functional theory (DFT) method. The micropore volume (V_{mic}) was obtained using the t-plot method. The average pore diameter (D_{ap}) of NHCAs was calculated by the equation of $D_{ap} = 4V_t/S_{BET}$.

2.3. Preparation of NHCA electrodes

Firstly, the electrodes for electrochemical measurements were prepared by mixing the NHCAs and polytetrafluoroethylene together with mass ratio of 9:1 in deionized water to obtain a slurry. Then, the slurry was rolled into thin film and cut into round films (12 mm in diameter). After drying in a vacuum oven at 120 °C for 2 h, each round film was weighted to be about 2.0 mg cm⁻². The electrode for electrochemical testing was prepared by firmly pressing the films onto nickel foams. Finally, a coin-type supercapacitor was assembled using two similar electrodes separated by a piece of polypropylene membrane with a 6 M KOH aqueous solution as the electrolyte. The cyclic voltammetry (CV) measurements were conducted on CHI760E electrochemical workstation (Chenhua, Shanghai, China). Electrochemical impedance spectra (EIS) were measured using an Ametek PARSTAT4000 electrochemistry workstation within a frequency range of 100 kHz to 0.01 Hz with 5 mV ac amplitude. The galvanostatic charge-discharge (GCD) measurements and cycle life tests were conducted on a supercapacitance test system (SCTs, Arbin Instruments, USA). The specific capacitance of the working electrodes was calculated from the galvanostatic discharge process via the following equation:

$$C_{cell} = \frac{I\Delta t}{m\Delta V} \quad (1)$$

$$C_s = \frac{2I'\Delta t}{m'\Delta V} = \frac{4I\Delta t}{m\Delta V} \quad (2)$$

where C_{cell} (F g⁻¹) is the specific capacitances of the symmetric supercapacitor, C_s (F g⁻¹) is the single electrode capacitance, m' and I' (A) represent the mass of single electrode and the relevant current, respectively, I (A) stands for the discharge current, m (g) is the total mass of the active material of the two-electrode cell, ΔV (V) and Δt (s) are the discharge voltage and the discharge time in the discharge process. The calculation of the density of activated carbon and volumetric specific capacitance was described in Supplementary Material.

The energy density (E, Wh kg⁻¹) and average power density (P, W kg⁻¹) of the supercapacitors were calculated based on the

following equations:

$$E = \frac{1}{2 \times 4 \times 3.6} C_s V^2 \quad (3)$$

$$P = \frac{E}{\Delta t} \quad (4)$$

where V (V) represents the working voltage (excluding IR drop), t (h) stands for the discharge time.

3. Results and discussion

Fig. 1 illustrates the overall construction process of NHCAs which is quite simple and straightforward. After heating petroleum asphalt and potassium citrate in inert atmosphere, the melted and fluid asphalt mixed with the potassium citrate uniformly. With the further increasing of temperature, the potassium citrate would decompose into potassium carbonate (Fig. S1) in the matrix of heated asphalt, serving as the in-situ templates which will guide the carbon source to form the scaffold of nanosheet-assembled architecture [20,22]. At higher temperature, the in-situ formed potassium carbonate is decomposed to produce carbon dioxide and potassium oxide. The carbon dioxide could etch the carbon to produce micropores [20]. Meanwhile, the potassium oxide can react with carbon to generate metallic potassium. The as-formed metallic potassium is highly effective in contributing to porosity as its possibility of intercalating into graphene layers, leading to disruption of the carbon microstructures [1]. Because of the simplicity, the carbon materials synthesized using this method are highly attractive for some scale applications, for example, energy storage. Moreover, the yield of carbon through this method increases significantly, much higher than that of the carbon materials obtained from direct carbonization of potassium citrate (Fig. S2).

The structure details of the as-prepared carbons are carefully investigated. Firstly, the morphologies of these carbon materials synthesized at different conditions are compared in Fig. 2. As shown in Fig. 2a, the direct pyrolysis of petroleum asphalt can only produce irregular bulk carbon particles. The introduction of potassium citrate can create macropores because of the in-situ templates generated through decomposing potassium citrate [20]. Fig. 2b–d exhibit the evolution of the macroporous architectures with the increase of potassium citrate. With two-fold of potassium citrate employed (Fig. 2b), the macropores-decorated bulk particles are produced and the pore-wall is quite thick. To further increase the ratio to four-fold, the wall-thick is significantly reduced (Fig. 2c and Fig. S3) and the nanosheet-wrapped nanocages are interconnected, giving rise to a desired scaffold for capacitive energy storage. At higher content of the potassium citrate in the mixture (Fig. 2d), the structures can be well-maintained whereas carbon fragments are also detected which may be due to the unmatched in-situ template and carbon precursor. As a reference, the morphology of the structure from direct pyrolysis of potassium

citrate (denoted as HCAs) has also been observed. As shown in Fig. S3c, the architecture contains macropores assembled by thick and thin nanosheet as well as fragments, which demonstrates poor controllability.

The structure of the NHCA-4 has been further investigated using TEM for more details. As shown in Fig. 3a, the remained carbon perfectly replicates the bulk morphology of the stacked templates and the removing templates could leave the interconnected porous networks behind, thus producing such an architecture. Moreover, the carbon shell thickness is quite thin which is almost transparent to the electron beams. Under higher resolution image (Fig. 3b), the thickness of the nanosheet is determined to be around 30 nm. Energy disperse X-ray (EDX) spectra have been recorded under TEM observation. As shown in Fig. 3c, a fairly high content of oxygen and a tiny amount of nitrogen have been detected except the main carbon element. These uniformly distributed heteroatoms can improve the wettability of the as-prepared carbon materials, which can thus facilitate the electrolyte transport among these nanosheet [30,31].

The chemical states of these heteroatoms have been further analyzed by XPS. As shown in Fig. 4a, the full spectra of the carbon architectures synthesized at different conditions are compared. Three kinds of peaks can be found which correspond to carbon, nitrogen and oxygen with the detailed results listed in Table S1. These results are in good agreement with EDX analysis. The high-resolution O1s spectrum of NHCA-4 (525–545 eV) is presented in Fig. 4b, where different types of O-containing groups could be verified on the surface of the as-prepared carbon, including C=O (531.9 eV), C–O (533.4 eV) and O–H (534.0 eV). It is well accepted that defects in the carbon materials play an important role in their electrochemical performance [32]. As a result, this property of the as-prepared NHCAs is investigated by Raman Spectrum. As shown in Fig. 4c, the intensity of D band (around 1350 cm^{-1}) associated with defects and G (around 1580 cm^{-1}) band corresponding to graphitic carbon [33] contributes to a relative large I_D/I_G ratio, indicating that all of the NHCAs are defect-rich carbon materials. Moreover, the XRD pattern of the NHCA-4 is displayed in Fig. 4d. Two broad peaks at 23.4° and 43.5° reveal the amorphous characteristics and the complete removal of potassium-containing residuals.

Other key properties, which are of particular importance for energy storage application, the specific surface and pore size distribution [34,35], have been carefully evaluated by nitrogen sorption isotherms. As shown in Fig. 4e, all of NHCAs display a type I isotherm based on the IUPAC classification, revealing the presence of a high content of micropores. At medium pressure, the small hysteresis loop in the isotherms of NHCAs disclose the existence of mesopores. The detailed pore structure parameters of the NHCAs samples are summarized in Table S2 where the specific surface area and pore volume increase in the same order, specifically, HCA ($786 \text{ m}^2 \text{ g}^{-1}$, $0.39 \text{ cm}^3 \text{ g}^{-1}$) < NHCA-2 ($836 \text{ m}^2 \text{ g}^{-1}$, $0.41 \text{ cm}^3 \text{ g}^{-1}$) < NHCA-4 ($1267 \text{ m}^2 \text{ g}^{-1}$, $0.53 \text{ cm}^3 \text{ g}^{-1}$) < NHCA-6 ($1437 \text{ m}^2 \text{ g}^{-1}$, $0.60 \text{ cm}^3 \text{ g}^{-1}$). Fig. 4f shows the pore size distribution

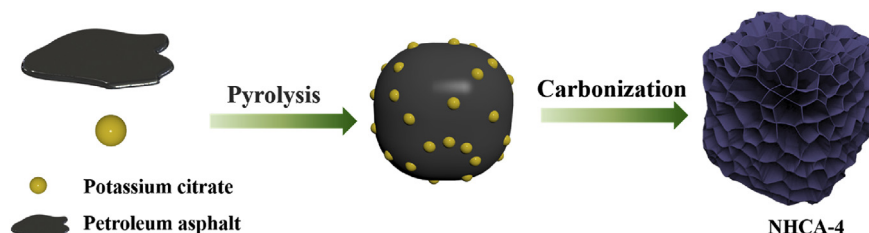


Fig. 1. Illustration of the construction process. (A colour version of this figure can be viewed online.)

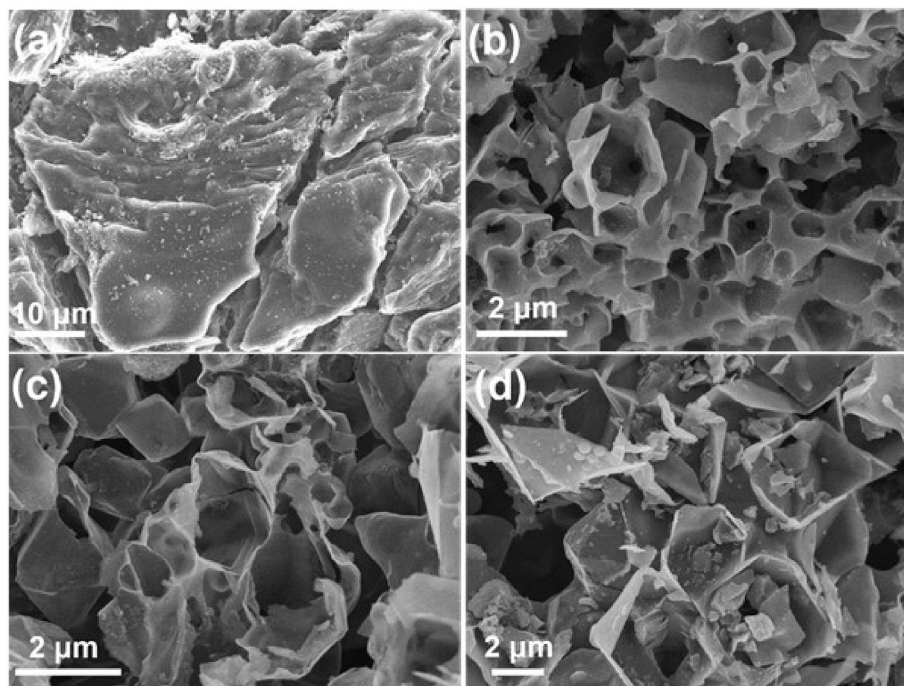


Fig. 2. SEM image of the (a) PAC, (b) NHCA-2, (c) NHCA-4, and (d) NHCA-6

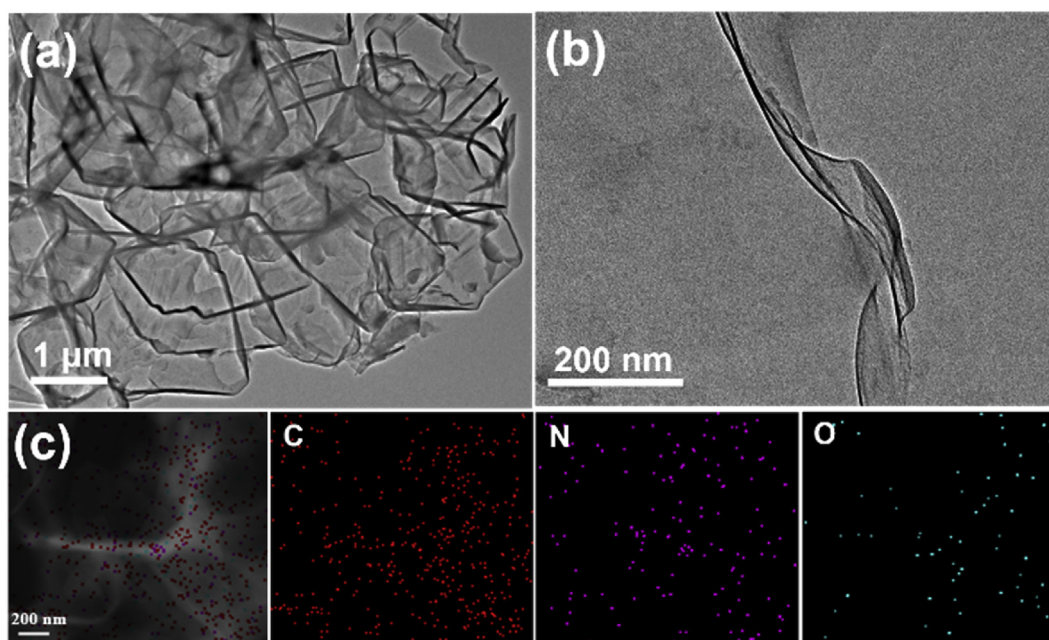


Fig. 3. (a) and (b) TEM images of NHCA-4. (c) Element mapping analysis of NHCA-4. (A colour version of this figure can be viewed online.)

curves of NHCAs, the bimodal distribution concentrates on ca. 0.6–1 nm and 1.2–2 nm.

The electrochemical performances of these NHCAs were evaluated using a two-electrode configuration with two identical electrodes separated by an ion-permeable separator in a 6 M KOH electrolyte. Fig. 5a compares the CV curves at a scan rate of 50 mV s^{-1} . Definitely, all the curves exhibit approximately rectangular shapes without distinct redox peaks, which demonstrate the ideal electrical double-layer capacitance behavior of NHCAs because of the reversible adsorption and desorption of the

electrolyte ions. Remarkably, NHCA-4 gives the largest rectangle at the same scan rate, revealing the largest specific capacitance. Meanwhile, the CV curve of the one synthesized by direct pyrolysis of potassium citrate affords a distorted rectangular shape with a much smaller area which indicates the synergetic effects of potassium citrate and petroleum asphalt in creating the hierarchical architectures. The power capability of the NHCA-4 has been further tested at scan rates ranging from 5 to 200 mV s^{-1} in Fig. 5b. The perfect rectangular shape of its CV curve can still be well maintained even at the scan rate as high as 200 mV s^{-1} , revealing its

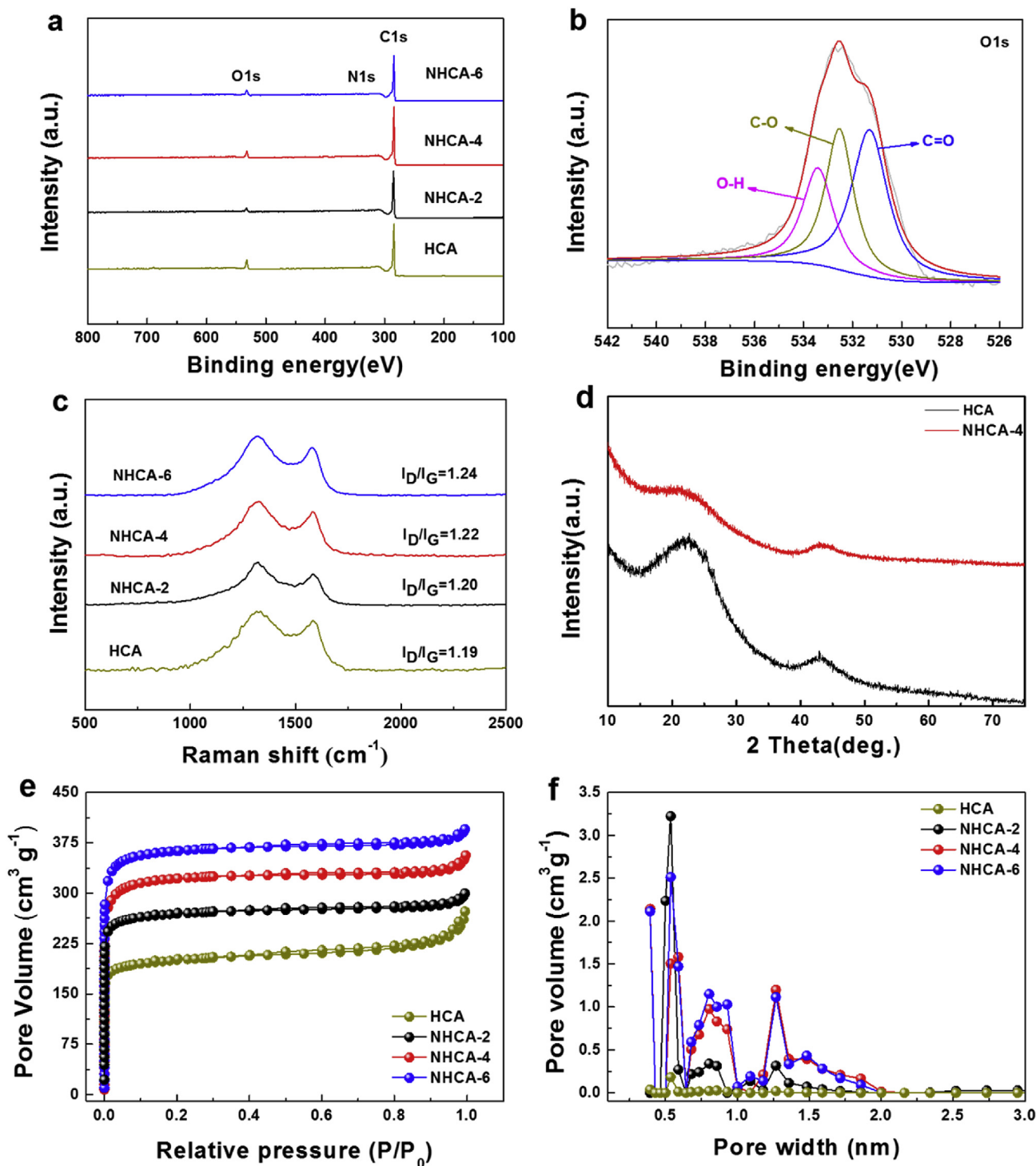


Fig. 4. (a) Full XPS spectra of HCA and NHCA. (b) O1s spectrum of NHCA-4. (c) Raman spectra and (d) XRD patterns of the HCA and NHCA. (e) N_2 adsorption-desorption isotherms of HCA and NHCA and their (f) pore size distributions. (A colour version of this figure can be viewed online.)

outstanding rate performance. The excellent capacitive capability has been further confirmed by Galvanostatic charge-discharge (GCD) measurements. Fig. 5c shows the GCD curves at 0.1 A g^{-1} . All the curves reveal equirural triangle shape in the potential range from 0 to 1.0 V, which manifests an ideal double layer capacitance behavior and is consistent with CV tests. Furthermore, these NHCA have extremely small IR drop, demonstrating their unique morphology in favor of extremely fast charge transfer. The specific

capacitance of the NHCA at different current densities is shown in Fig. 5d. As shown, the gravimetric specific capacitance of HCA, NHCA-2, NHCA-4 and NHCA-6 electrode is 152 F g^{-1} , 196 F g^{-1} , 307 F g^{-1} and 236 F g^{-1} at 0.05 A g^{-1} , respectively. It is worth noting that the gravimetric capacitance of NHCA-4 electrode is also superior to many other related nanostructured carbon reported elsewhere (Table S3) [36–41]. The volumetric specific capacitance is 60 F cm^{-3} , 70 F cm^{-3} , 93 F cm^{-3} and 67 F cm^{-3} at 0.05 A g^{-1} for

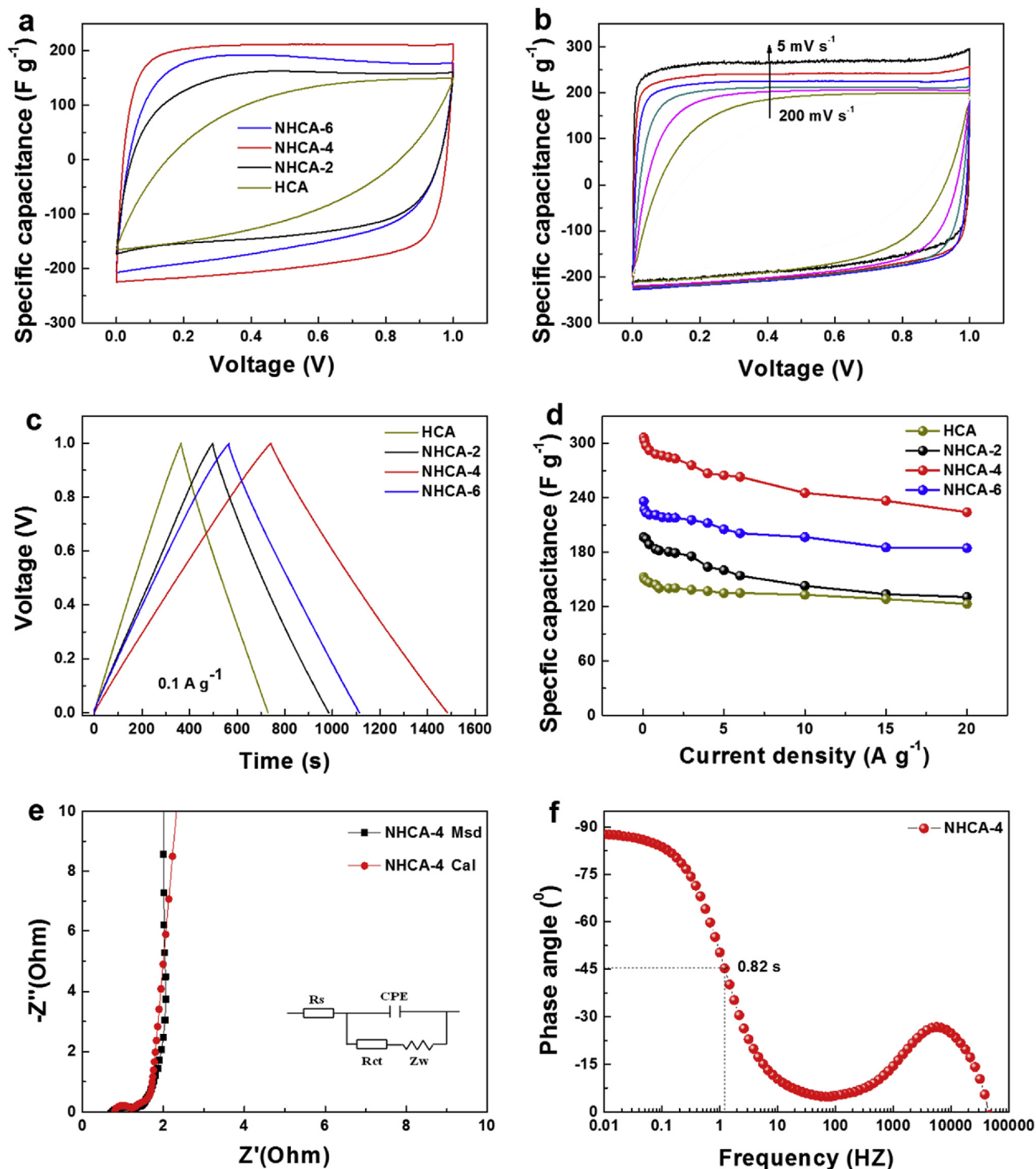


Fig. 5. (a) CV curves of HCA and NHCA-2, -4, -6 at scan rate of 50 mV s⁻¹. (b) CV curve of NHCA-4 at scan rates ranging from 5 to 200 mV s⁻¹. (c) GCD curves of HCA and NHCA-2, -4, -6 at a current density of 0.1 A g⁻¹. (d) The rate performances of HCA and NHCA-2, -4, -6. (e) The Nyquist plots (insert was the equivalent circuit model) and (f) the Bode plot of NHCA-4. (A colour version of this figure can be viewed online.)

HCA, NHCA-2, NHCA-4 and NHCA-6, respectively, according to Table S4, which is compared favourably to commercial one (Table S5). The outstanding performance of NHCA-4 can be ascribed to its unique structure. The macropores in the architecture serve as a reservoir holding electrolytes while the meso-/micropores decorated nanosheet can essentially reduce the diffusion length for ions as well as provide sufficient accommodation sites for ions. The

rational combination of different size pores with disparate functions can thus allow sufficiently large amount of ions be adsorbed/desorbed in an extremely fast manner. To further explain the outstanding electrochemical performance of the NHCA-4, the impedance measurement was conducted in the frequency ranging from 10⁵ Hz to 10⁻² Hz with 5 mV ac amplitude and shown in Fig. 5e. The measured Nyquist plot (black one, Msd) consists of

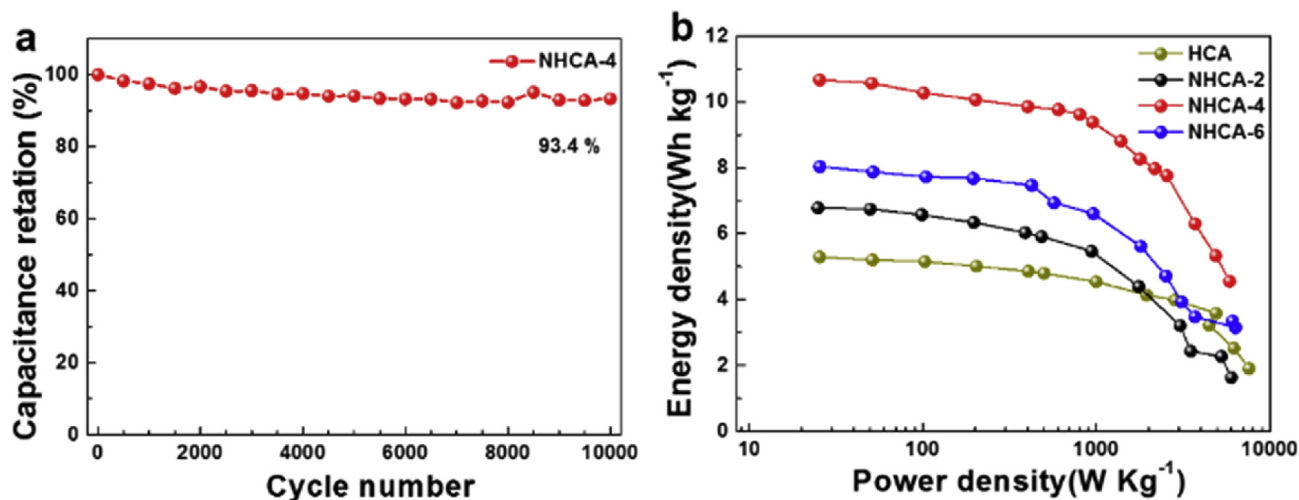


Fig. 6. (a) Cycle stability of NHCA-4 electrodes at 5 A g^{-1} . (b) The Ragone plots of the HCA and NHCAs at 6 M KOH electrolyte. (A colour version of this figure can be viewed online.)

semicircles at high frequency region and vertical lines at low frequency range, indicative of the low intrinsic resistance and ideal capacitance behavior. As compared (Fig. S4), the NHCA-4 gives the smallest intrinsic ohmic resistance (R_s) and charge transfer resistance (R_{ct}), demonstrating that NHCA-4 possesses superior electrical conductivity and the fastest charge transfer rate. To quantitatively evaluate the electrode resistance, equivalent circuit model is introduced and displayed in Fig. 5e (C_{ad}). Obviously, the M_{sd} and C_{ad} plots are almost overlapped with each other, revealing the constructed model can perfectly reflect the characteristics of the as-prepared supercapacitors. The calculated value of each circuit component is listed in Table S6. To further explain the capacitance behavior, Bode plots were introduced and shown in Fig. 5f. The phase angle of NHCA-4 (-87.7°) gives the smallest deviation to the ideal electric double layer capacitors (-90°), revealing the extraordinary capacitive behavior, which corresponds well with the other electrochemical measurements. The time constant τ_0 is 0.82 s and the small value is due to the unique architecture.

The cyclic stability of the NHCA-4 was conducted at a current density of 5 A g^{-1} for 10000 cycles. Fig. 6a shows that capacitance retention is as high as 93.4%, demonstrating its excellent reversibility and outstanding structural stability. The cycling stability of other two NHCAs is shown in Fig. S5, which is inferior to NHCA-4. The Ragone plots of different NHCAs in 6 M KOH electrolyte have been listed in Fig. 6b. Among them, NHCA-4 delivers the highest energy density, reaching 10.7 Wh kg^{-1} at 25.5 W kg^{-1} and remaining 4.5 Wh kg^{-1} at 5854 W kg^{-1} . The good electrochemical performance of NHCAs is mainly ascribed to the unique structure of the three-dimensional porous carbon materials, which not only significantly speeds up the electron transfer via shortening the ion diffusion distance, but also enhance the rate capacitance through its ion-buffering reservoir feature.

4. Conclusions

In summary, a green and scalable method to produce hierarchical porous carbons has been proposed through carbonizing petroleum asphalt in the presence of potassium citrate. The potassium citrate serves as not only the in-situ template for scaffold construction but also as the environment-friendly activation agents for pore regulation. Because of the simplicity and straightforwardness as well as the cheap precursors employed, the strategy suggested here may hold great potential for industrially scalable production in

a sustainable manner. The as-prepared carbon architectures show large specific surface area and hierarchical porosity with rationally combined pores. As a result, an outstanding electrochemical performance as electrode materials for supercapacitors has been delivered. More specifically, a large specific capacitance of 307 F g^{-1} at a current density of 0.05 A g^{-1} is delivered and attractive capacitance retention is afforded both at high rates and long cycles. The novel strategy proposed here may be of great importance for green production of high-performance carbon-based electrode materials.

Acknowledgments

The authors acknowledge the support from the Fundamental Research Funds for the Central Universities (15 C \times 08005 A), the Financial Support from Taishan Scholar Project (No. ts201712020), Technological Leading Scholar of 10000 Talent Project (No. W03020508), Shandong Provincial Natural Science Foundation (ZR2018ZC1458), China.

Appendix A. Supplementary data

Supplementary data to this article can be found online at <https://doi.org/10.1016/j.carbon.2019.06.059>.

References

- [1] L. Wang, J. Han, D. Kong, Y. Tao, Q.-H. Yang, Enhanced roles of carbon architectures in high-performance lithium-ion batteries, *Nano-Micro Lett.* 11 (2019) 5.
- [2] X. Li, B.Y. Guan, S. Gao, X.W. Lou, A general dual-templating approach to biomass-derived hierarchically porous heteroatom-doped carbon materials for enhanced electrocatalytic oxygen reduction, *Energy Environ. Sci.* 12 (2019) 648–655.
- [3] K. Jayaramulu, D.P. Dubal, B. Nagar, V. Ranc, O. Tomanec, M. Petr, K.K.R. Datta, et al., Ultrathin hierarchical porous carbon nanosheets for high-performance supercapacitors and redox electrolyte energy storage, *Adv. Mater.* 30 (2018) 1705789.
- [4] X. Deng, B. Zhao, L. Zhu, Z. Shao, Molten salt synthesis of nitrogen-doped carbon with hierarchical pore structures for use as high-performance electrodes in supercapacitors, *Carbon* 93 (2015) 48–58.
- [5] C. Long, L. Jiang, X. Wu, Y. Jiang, D. Yang, C. Wang, et al., Facile synthesis of functionalized porous carbon with three-dimensional interconnected pore structure for high volumetric performance supercapacitors, *Carbon* 93 (2015) 412–420.
- [6] D. Zhu, Y. Wang, W. Lu, H. Zhang, Z. Song, D. Luo, et al., A novel synthesis of hierarchical porous carbons from interpenetrating polymer networks for high performance supercapacitor electrodes, *Carbon* 111 (2017) 667–674.

- [7] Z. Li, J.T. Zhang, Y.M. Chen, J. Li, X.W. Lou, Pie-like electrode design for high-energy density lithium–sulfur batteries, *Nat. Commun.* 6 (2015) 8850.
- [8] J. Lang, X. Zhang, B. Liu, R. Wang, J. Chen, X. Yan, The roles of graphene in advanced Li-ion hybrid supercapacitors, *J. Energy Chem.* 27 (2018) 43–56.
- [9] R. Raccichini, A. Varzi, S. Passerini, B. Scrosati, The role of graphene for electrochemical energy storage, *Nat. Mater.* 14 (2015) 271–279.
- [10] Y. Dong, M. Yu, Z. Wang, Y. Liu, X. Wang, Z. Zhao, J. Qiu, A top-down strategy toward 3D carbon nanosheet frameworks decorated with hollow nanostructures for superior lithium storage, *Adv. Funct. Mater.* 26 (2016) 7590–7598.
- [11] D.W. Wang, F. Li, M. Liu, G.Q. Lu, H.M. Cheng, 3D aperiodic hierarchical porous graphitic carbon material for high-rate electrochemical capacitive energy storage, *Angew. Chem. Int. Ed.* 48 (2009), 1525–1525.
- [12] J. Zhao, Y.F. Jiang, H. Fan, M. Liu, O. Zhuo, X.Z. Wang, et al., Porous 3D few-layer graphene-like carbon for ultrahigh-power supercapacitors with well-defined structure–performance relationship, *Adv. Mater.* 29 (2017) 1604569.
- [13] J. Zhang, X.S. Zhao, On the configuration of supercapacitors for maximizing electrochemical performance, *ChemSusChem* 5 (2012) 818–841.
- [14] C.Z. Yuan, B. Gao, L.F. Shen, S.D. Yang, L. Hao, X.J. Lu, et al., Hierarchically structured carbon-based composites: design, synthesis and their application in electrochemical capacitors, *Nanoscale* 3 (2011) 529–545.
- [15] R.-W. Fu, Z.-H. Li, Y.-R. Liang, F. Li, F. Xu, D.-C. Wu, Hierarchical porous carbons: design, preparation, and performance in energy storage, *N. Carbon Mater.* 26 (2011) 171–179.
- [16] K. Xie, X. Qin, X. Wang, Y. Wang, H. Tao, Q. Wu, et al., Carbon nanocages as supercapacitor electrode materials, *Adv. Mater.* 24 (2012) 347–352.
- [17] Z. Ling, Z. Wang, M. Zhang, C. Yu, G. Wang, J. Qiu, et al., Sustainable synthesis and assembly of biomass-derived B/N Co-doped carbon nanosheets with ultrahigh aspect ratio for high-performance supercapacitors, *Adv. Funct. Mater.* 26 (2016) 111–119.
- [18] S. Xiong, J. Fan, Y. Wang, J. Zhu, J. Yu, Z. Hu, A facile template approach to nitrogen-doped hierarchical porous carbon nanospheres from polydopamine for high-performance supercapacitors, *J. Mater. Chem.* 5 (2017) 18242–18252.
- [19] D. Guo, R. Xin, Z. Zhang, W. Jiang, G. Hu, M. Fan, N-doped hierarchically micro- and mesoporous carbons with superior performance in supercapacitors, *Electrochim. Acta* 291 (2018) 103–113.
- [20] M. Sevilla, A.B. Fuertes, Direct synthesis of highly porous interconnected carbon nanosheets and their application as high-performance supercapacitors, *ACS Nano* 8 (2014) 5069–5078.
- [21] B. Yang, J. Chen, S. Lei, R. Guo, H. Li, S. Shi, X. Yan, Spontaneous growth of 3D framework carbon from sodium citrate for high energy- and power-density and long-life sodium-ion hybrid capacitors, *Adv. Energy Mater.* 8 (2018) 1702409.
- [22] D.P. Li, X.H. Ren, Q. Ai, Q. Sun, L. Zhu, Y. Liu, et al., Facile fabrication of nitrogen-doped porous carbon as superior anode material for potassium-ion batteries, *Adv. Energy Mater.* 8 (2018) 1802386.
- [23] H.S. Hou, X.Q. Qiu, W.F. Wei, Y. Zhang, X.B. Ji, Carbon anode materials for advanced sodium-ion batteries, *Adv. Energy Mater.* 7 (2017) 1602898.
- [24] D. Saurel, B. Orayech, B. Xiao, D. Carriazo, X. Li, T. Rojo, From charge storage mechanism to performance: a roadmap toward high specific energy sodium-ion batteries through carbon anode optimization, *Adv. Energy Mater.* 8 (2018) 1703268.
- [25] Q. Zhang, J.-Q. Huang, M.-Q. Zhao, W.-Z. Qian, F. Wei, Carbon nanotube mass production: principles and processes, *ChemSusChem* 4 (2011) 864–889.
- [26] J.Y. Liu, Y. Liu, P. Li, L.H. Wang, H.R. Zhang, H. Liu, et al., Z.T. Li Wang, M.B. Wu, Fe-N-doped porous carbon from petroleum asphalt for highly efficient oxygen reduction reaction, *Carbon* 126 (2018) 1–8.
- [27] S.H. Choi, G. Nam, S. Chae, D. Kim, N. Kim, W.S. Kim, et al., Robust pitch on silicon nanolayer-embedded graphite for suppressing undesirable volume expansion, *Adv. Energy Mater.* 9 (2019) 1803121.
- [28] Y.X. Lu, C.L. Zhao, X.G. Qi, Y.R. Qi, H. Li, X.J. Huang, et al., Pre-oxidation-tuned microstructures of carbon anodes derived from pitch for enhancing Na storage performance, *Adv. Energy Mater.* 8 (2018) 1800108.
- [29] Y. Li, L. Mu, Y.-S. Hu, H. Li, L. Chen, X. Huang, Pitch-derived amorphous carbon as high performance anode for sodium-ion batteries, *Energy Storage Mater* 2 (2016) 139–145.
- [30] S. Li, C. Yu, J. Yang, C. Zhao, M. Zhang, J. Qiu, et al., A superhydrophilic "nanogel" for stabilizing metal hydroxides onto carbon materials for high-energy and ultralong-life asymmetric supercapacitors, *Energy Environ. Sci.* 10 (2017) 1958–1965.
- [31] Y. Song, J. Yang, K. Wang, S. Haller, Y. Wang, C. Wang, et al., In-situ synthesis of graphene/nitrogen-doped ordered mesoporous carbon nanosheet for supercapacitor application, *Carbon* 96 (2016) 955–964.
- [32] J. Zhu, A.S. Childress, M. Karakaya, S. Dandeliya, A. Srivastava, Y. Lin, et al., Defect-engineered graphene for high-energy- and high-power-density supercapacitor devices, *Adv. Mater.* 28 (2016) 7185–7192.
- [33] H. Hu, J. Zhang, B. Guan, X.W. Lou, Unusual formation of CoSe@carbon nanoboxes, which have an inhomogeneous shell, for efficient lithium storage, *Angew. Chem. Int. Ed.* 55 (2016) 9514–9518.
- [34] J. Chmiola, G. Yushin, Y. Gogotsi, C. Portet, P. Simon, P.L. Taberna, Anomalous increase in carbon capacitance at pore sizes less than 1 nanometer, *Science* 313 (2006) 1760–1763.
- [35] Y.W. Zhu, S. Murali, M.D. Stoller, K.J. Ganesh, W.W. Cai, P.J. Ferreira, et al., Carbon-based supercapacitors produced by activation of graphene, *Science* 332 (2011) 1537–1541.
- [36] Z.-Q. Hao, J.-P. Cao, Y. Wu, X.-Y. Zhao, Q.-Q. Zhuang, X.-Y. Wang, et al., Preparation of porous carbon sphere from waste sugar solution for electric double-layer capacitor, *J. Power Sources* 361 (2017) 249–258.
- [37] B. Liu, M. Yang, H. Chen, Y. Liu, D. Yang, H. Li, Graphene-like porous carbon nanosheets derived from salvia splendens for high-rate performance supercapacitors, *J. Power Sources* 397 (2018) 1–10.
- [38] Y.K. Kim, J.H. Park, J.W. Lee, Facile nano-templated CO₂ conversion into highly interconnected hierarchical porous carbon for high-performance supercapacitor electrodes, *Carbon* 126 (2018) 215–224.
- [39] J. Pang, W. Zhang, J. Zhang, G. Cao, M. Han, Y. Yang, Facile and sustainable synthesis of sodium lignosulfonate derived hierarchical porous carbons for supercapacitors with high volumetric energy densities, *Green Chem.* 19 (2017) 3916–3926.
- [40] Z. Liu, Y. Zeng, Q. Tang, A. Hu, K. Xiao, S. Zhang, et al., Potassium vapor assisted preparation of highly graphitized hierarchical porous carbon for high rate performance supercapacitors, *J. Power Sources* 361 (2017) 70–79.
- [41] D. Zhu, Y. Wang, W. Lu, H. Zhang, Z. Song, D. Luo, et al., A novel synthesis of hierarchical porous carbons from interpenetrating polymer networks for high performance supercapacitor electrodes, *Carbon* 111 (2017) 667–674.